



HAL
open science

VLTI/VINCI observations of the nucleus of NGC 1068 using the adaptive optics system MACAO

Markus Wittkowski, Pierre Kervella, Robin Arsenault, Francesco Paresce, T. Beckert, Gerd Weigelt

► **To cite this version:**

Markus Wittkowski, Pierre Kervella, Robin Arsenault, Francesco Paresce, T. Beckert, et al.. VLTI/VINCI observations of the nucleus of NGC 1068 using the adaptive optics system MACAO. *Astronomy & Astrophysics* - A&A, 2004, 418, pp.L39-L42. <hal-03724084>

HAL Id: hal-03724084

<https://hal.science/hal-03724084v1>

Submitted on 17 Jul 2022

HAL is a multi-disciplinary open access archive for the deposit and dissemination of scientific research documents, whether they are published or not. The documents may come from teaching and research institutions in France or abroad, or from public or private research centers.

L'archive ouverte pluridisciplinaire **HAL**, est destinée au dépôt et à la diffusion de documents scientifiques de niveau recherche, publiés ou non, émanant des établissements d'enseignement et de recherche français ou étrangers, des laboratoires publics ou privés.



HAL Authorization

VLT/VINCI observations of the nucleus of NGC 1068 using the adaptive optics system MACAO[★]

M. Wittkowski¹, P. Kervella^{1,2}, R. Arsenault¹, F. Paresce¹, T. Beckert³, and G. Weigelt³

¹ European Southern Observatory, Karl Schwarzschild-Str. 2, 85748 Garching, Germany

² LESIA, Observatoire de Paris, 92195 Meudon Cedex, France

³ Max-Planck-Institut für Radioastronomie, Auf dem Hügel 69, 53121 Bonn, Germany

Received 8 March 2004 / Accepted 20 March 2004

Abstract. We present the first near-infrared *K*-band long-baseline interferometric measurement of the nucleus of the prototype Seyfert 2 Galaxy NGC 1068 with resolution $\lambda/B \sim 10$ mas obtained with the Very Large Telescope Interferometer (VLT) and the two 8.2 m diameter Unit Telescopes UT 2 and UT 3. The adaptive optics system MACAO (Multi Application Curvature Adaptive Optics) was employed to deliver wavefront-corrected beams to the *K*-band commissioning instrument VINCI. A squared visibility amplitude of $16.3 \pm 4.3\%$ was measured for NGC 1068 at a sky-projected baseline length of 45.8 m and azimuth angle 44.9 deg. This value corresponds to a *FWHM* of the *K*-band intensity distribution of 5.0 ± 0.5 mas (0.4 ± 0.04 pc at the distance of NGC 1068) if it consists of a single Gaussian component. Taking into account *K*-band speckle interferometry observations (Wittkowski et al. 1998; Weinberger et al. 1999; Weigelt et al. 2004), we favor a multi-component model for the intensity distribution where a part of the flux originates from scales clearly smaller than ~ 5 mas ($\lesssim 0.4$ pc), and another part of the flux from larger scales. The *K*-band emission from the small ($\lesssim 5$ mas) scales might arise from substructure of the dusty nuclear torus, or directly from the central accretion flow viewed through only moderate extinction.

Key words. techniques: interferometric – galaxies: nuclei – galaxies: Seyfert – galaxies: individual: NGC 1068

1. Introduction

The Seyfert galaxy NGC 1068 harbors one of the brightest and closest active galactic nuclei (AGN). Active galaxies appear as types 1 and 2, where the spectra of the former exhibit broad and narrow emission lines, and those of the latter show only narrow lines. Antonucci & Miller (1985) suggested that the broad-line emission regions are located inside an optically and geometrically thick disk and that central continuum and broad-line photons are scattered into the line-of-sight by free electrons above and below the disk. Depending on the observer's viewing angle, the broad-line emission region is either obscured or not. This suggestion is now widely accepted and has evolved to the so-called “unified scheme of AGN” (e.g., Antonucci 1993).

Various theoretical models of the postulated dusty tori have been presented by, for instance, Krolik & Begelman (1988), Pier & Krolik (1992), Granato & Danese (1994), Efstathiou & Rowan Robinson (1995), Manske et al. (1998), Nenkova et al. (2002), and Vollmer et al. (2004). Owing to the lack of spatially resolved observations, the models were usually compared to the integrated spectrum of the core of NGC 1068. It turned out that torus models with a wide variety of geometries, spatial extensions, and optical depths are consistent with this spectrum. In addition, the nature of the central emission source

itself could not be well constrained because the flux spectrum of the very inner nuclear engine could not be separated from the emission of surrounding material.

Several high-resolution infrared observations of NGC 1068 showing a compact central IR core and surrounding structure were carried out by, for instance, Thatte et al. (1997), Rouan et al. (1998), Wittkowski et al. (1998), Weinberger et al. (1999), and Bock et al. (2000). Wittkowski et al. (1998) presented both a *K*-band visibility function up to spatial frequencies corresponding to a baseline of 6 m, as well as the first 76 mas resolution *K*-band image of the nucleus of NGC 1068 obtained by bispectrum speckle interferometry. The compact central IR core was resolved with a Gaussian *FWHM* of ~ 30 mas (2 pc). New *K*-band and *H*-band bispectrum speckle interferometry observations were performed by Weigelt et al. (2004).

Very recently, the first interferometers consisting of 8–10 m class telescopes started operations, and they have already succeeded in observing AGN with much higher spatial resolutions. The potential of optical/infrared interferometry to investigate AGN was recently discussed by Wittkowski et al. (2003). Swain et al. (2003) reported the first *K*-band interferometric observations of the Seyfert 1 galaxy NGC 4151 obtained with the 85 m baseline of the Keck Interferometer. Jaffe et al. (2004) reported on the first mid-infrared interferometric observation of the dusty torus of NGC 1068 using VLT/MIDI.

In the present letter, we report on the first *K*-band long-baseline interferometric observation of NGC 1068.

Send offprint requests to: M. Wittkowski,
e-mail: mwi@tkow@eso.org

[★] Based on public commissioning data released from the VLT (www.eso.org/projects/vlti/instru/vinci/vinci_data_sets.html).

Table 1. Calibration sequence of NGC 1068. JD is the Julian date of the observation, N the number of processed interferograms, B and A_z the projected baseline length and azimuth angle (east of north), and μ^2 the obtained coherence factors with their statistical errors. The interferometric efficiency (IE) given in italic characters is the value adopted for the calibration of the NGC 1068 data.

JD	N	B (m)	A_z	$\mu^2 \pm \text{stat.}$	IE $\pm \text{stat.} \pm \text{syst.}$	$V^2 \pm \text{stat.} \pm \text{syst.}$	Target
2 452 948.717	250	45.79	44.87	0.054 ± 0.017	<i>$0.340 \pm 0.009 \pm 0.001$</i>	$0.158 \pm 0.049 \pm 0.001$	NGC 1068
2 452 948.722	214	46.00	45.13	0.062 ± 0.031	<i>$0.340 \pm 0.009 \pm 0.001$</i>	$0.182 \pm 0.091 \pm 0.001$	NGC 1068
2 452 948.761	407	46.62	45.40	0.319 ± 0.005	$0.348 \pm 0.006 \pm 0.001$		HD 20356
2 452 948.767	438	46.64	45.62	0.304 ± 0.005	$0.331 \pm 0.005 \pm 0.001$		HD 20356
2 452 948.772	416	46.63	45.80	0.315 ± 0.006	$0.344 \pm 0.007 \pm 0.001$		HD 20356

2. Observations and data reduction

The NGC 1068 interferometric data were obtained with the Very Large Telescope Interferometer (VLTI) and the K -band commissioning instrument VINCI (Kervella et al. 2000, 2003), used with the fiber-based beam combiner MONA, on Nov. 4, 2003. The UT2-UT3 baseline with 47 m ground length was used. Both telescopes were equipped with the Multi Application Curvature Adaptive Optics (MACAO) system. These data were taken in the framework of the commissioning of MACAO-VLTI.

MACAO systems. For a detailed description of the MACAO systems see Arsenault et al. (2003). The MACAO systems are four curvature adaptive optics systems installed at the Coudé focus of each UT (the systems for UTs 1 and 4 will be installed in the fall of 2004 and first quarter of 2005). The Coudé train mirror M8 is replaced by a 60 actuator bimorph deformable mirror in a tip-tilt mount. The mirror M9 is a dichroic which transmits visible light to the wavefront sensor and reflects the wavelength range from 1 to 13 μm to the VLTI recombination laboratory. During commissioning, the two MACAO systems on UTs 2 and 3 showed very similar and consistent results. Strehl ratios of 65% were obtained on bright guide stars ($V < 11$) under optical seeing conditions of up to 0.8". On fainter sources with V magnitudes of 14.5 and 16, Strehl ratios of 45% (seeing 0.60") and 25% (seeing 0.55") were obtained, respectively. For use with the single-mode fiber instrument VINCI, a high Strehl ratio ensures a high concentration of light onto the 56 mas diameter fiber core of VINCI, hence allowing the interferometric observation of faint sources such as NGC 1068. For both MACAO-VLTI systems the reference source was the nucleus of NGC 1068 itself, and the same control parameters were used for both AO systems. No neutral density filters were used, the main loop gain was 0.50. The optical seeing at the time of observation was $\sim 0.9''$. It is difficult to estimate the MACAO performance for our NGC 1068 observations since the source is extended and an acquisition image could not be taken.

Interferometric data. 1000 interferograms of the nucleus of NGC 1068 were obtained in two series of 500 scans. The fringe frequency was 216 Hz, a compromise between faint object sensitivity and immunity to the atmospheric piston effect. Of the recorded interferograms, 464 were processed successfully by the VINCI data reduction software as described by

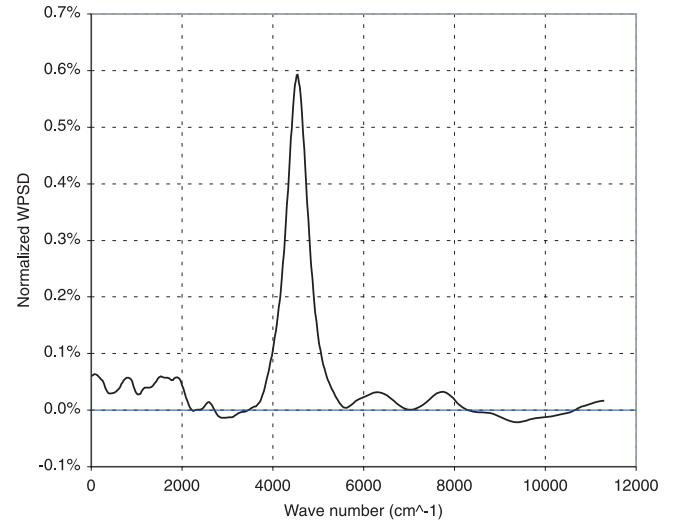


Fig. 1. Average wavelets power spectral density (WPSD) of the 464 processed interferograms of NGC 1068. The subtraction of the background noise from the processed fringes' power peak left no residual bias on the final WPSD. The power integration is done between wave numbers 2000 and 8000 cm^{-1} .

Kervella et al. (2004). Table 1 lists the observational details for the NGC 1068 and the calibrator data, as well as the resulting visibility values. Figure 1 shows the background- and noise-corrected average wavelet power spectral density of the NGC 1068 interferograms. The fringes' power peak around wave number 4500 cm^{-1} is not affected by any significant power spectrum bias, despite the faintness of the source. The effective wavelength of the NGC 1068 observations is approximately 2.18 μm . The K5 giant HD 20356 ($\theta_{\text{UD}} = 1.81 \pm 0.02 \text{ mas}$) from Cohen et al. (1999) and Bordé et al. (2002) was used as calibration star (effective wavelength $\lambda = 2.181 \mu\text{m}$). Observational parameters and data reduction of the calibration star were identical to those of NGC 1068. The systematic error induced by the calibrator on the final visibility values is negligible compared to the statistical error. A calibrated squared visibility of $V^2 = 16.3 \pm 4.3\%$ for NGC 1068 was obtained for a sky-projected baseline with length $B = 45.839 \text{ m}$ and azimuth angle $A_z = 44.93 \text{ deg}$ (east of north).

Photometric estimate. Any photometric estimates using a single-mode fiber instrument is, in general, difficult due to the large and rapid fluctuations of the coupling of the object

light into the fiber core. However, the MACAO systems keep a large fraction of the object light inside the Airy disk, stabilize the injected flux, and a photometric estimate can be attempted. For commissioning purposes, a number of stars of various K -band magnitudes were observed on Nov. 3–5, 2003 with the same VLTI configuration as used for our NGC 1068 observations. The relation between the observed flux values and the K -band magnitudes m_K is consistent with the expected exponential function, so that the attempt of an absolute photometric calibration is reasonable. The best-fit relations between m_K and the photometric fluxes P_A and P_B (in ADU/s) are $P_A = 3.50 \times 10^6 \exp(-0.906 m_K)$ and $P_B = 1.46 \times 10^6 \exp(-0.901 m_K)$. The residual dispersions on m_K are $\sigma_A = 0.5$ mag and $\sigma_B = 0.6$ mag.

Since the performance, i.e. the Strehl ratio, of the MACAO systems for our extended source NGC 1068 is unknown, but very likely lower than that of the single bright stars (see above), the application of this photometric estimate on NGC 1068 can only give us a lower limit of the NGC 1068 flux in our field of view (FOV) of $F_K \geq 130 \pm 60$ mJy ($m_K \leq 9.2 \pm 0.4$). The size of the K -band Airy disk of the UTs with MACAO is 56 mas. In the absence of atmospheric turbulence, the FOV of our measurements would correspond exactly to the projection of the single-mode fiber on the sky. As this mode is matched by design to the diffraction pattern of the UTs, the effective $FWHM$ of our FOV would also be 56 mas. In practice, however our FOV is slightly larger due to the presence of residual uncorrected speckles, i.e. the limited Strehl ratio.

3. Discussion

Intensity distribution of the K -band emission. Our measured VLTI/VINCI K -band squared visibility amplitude of $|V|^2 = 16.3 \pm 4.3\%$ at a projected baseline length of $B = 45.8$ m corresponds to a single-component Gaussian intensity distribution with $FWHM$ 5.0 ± 0.5 mas (taking into account the VINCI broad-band K filter). With the distance to NGC 1068 of 14.4 Mpc (Bland-Hawthorn et al. 1997), this corresponds to a linear $FWHM$ of 0.4 ± 0.04 pc. This means that the VLTI/VINCI visibility value is consistent with a multi-component model only if at least 40% ($|V| = 40.4\%$) of the flux (i.e. ≥ 50 mJy) originates from scales ≤ 5 mas (Gaussian $FWHM \leq 6.7$ mas or ≤ 0.51 pc at the 3σ level).

The K -band visibility values obtained by speckle interferometry at spatial frequencies up to a baseline of 6–10 m (Wittkowski et al. 1998: SAO 6 m telescope; Weinberger et al. 1999: Keck 10 m; Weigelt et al. 2004: SAO 6 m) are consistent with a single-component Gaussian intensity distribution with azimuthally averaged $FWHM \sim 30$ mas (up to $B = 6$ m; Wittkowski et al. 1998), and also with a larger ~ 30 – 50 mas component plus a much smaller (unresolved) component (Weinberger et al. 1999; Weigelt et al. 2004).

The comparison of the visibility measurements obtained by these different methods is difficult since the visibility scales with the total observed flux in each FOV. However, since the speckle measurements show a structure with $FWHM \sim 30$ – 50 mas, and the VLTI/VINCI FOV is ~ 56 mas, the total flux

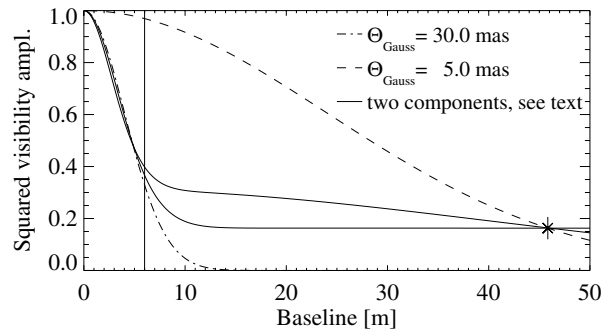


Fig. 2. Synthetic squared visibility function for (dashed line) a 5 mas Gaussian, (dashed-dotted line) a 30 mas Gaussian, and (solid lines) two examples for a two-component model where (upper line/lower line) 56%/40% of the total flux comes from a 3 mas/0.1 mas Gaussian and the remaining 44%/60% from a 54 mas/42 mas Gaussian ($FWHM$ values). Measurements are available for baselines $B = 46$ m reported in this letter (marked by the \times -symbol with error bar) and up to $B = 6$ – 10 m (Wittkowski et al. 1998; Weinberger et al. 1999; Weigelt et al. 2004). Both measurements are only matched if the small component has a size clearly below ~ 5 mas and if only part of the total flux in our FOV arises from this ≤ 5 mas component, and another part from a larger component. It is assumed that the FOV is the same for all shown models.

observed by VLTI/VINCI is very similar to that of the compact ~ 30 – 50 mas speckle component.

Both, the VLTI/VINCI and the speckle measurements are consistent with a multi-component intensity distribution where ≥ 50 mJy originate from scales ≤ 5 mas or ≤ 0.4 pc (VLTI/VINCI), and another part of the flux from larger scales of the order of 40 mas or 3 pc (speckle). Figure 2 shows the visibility models for a 5 mas Gaussian matching our VLTI/VINCI measurement, a 30 mas Gaussian matching the speckle measurements up to $B = 6$ m, and two examples for two-component models matching both, VLTI/VINCI and speckle measurements. It illustrates that two-component models are consistent with both measurements only if the small component has a size clearly below ~ 5 mas and a flux contribution of clearly less than the total flux in our FOV.

In the following, we discuss the possible origin of the newly constrained very compact (≤ 5 mas) K -band component.

Sources of very compact K -band emission. Dust at the inner cavity of the torus is heated to near the sublimation temperature of about 1000–1500 K and emits thermal K -band photons. These photons could escape in a direction other than the equatorial plane into our line-of-sight. Depending on the adopted dust properties and luminosity of the central source, the sublimation radius could be as small as about 0.3 pc (Barvainis et al. 1987; Thatte et al. 1997), or may as well be of the order of 1 pc or above (Dopita et al. 1998). Hence, the size of the inner dust cavity seems to be larger than our observed scale of $FWHM$ clearly below ~ 0.4 pc. It may more likely coincide with the scale of the ~ 40 mas (~ 3 pc) speckle component. However, since the work of Krolik & Begelman (1988) it has been discussed that the dusty torus very likely does not have a smooth uniform shape but may consist of a large number of clumps (Nenkova et al. 2002; Vollmer et al. 2004).

Vollmer et al. (2004) give a theoretical estimate for the radius of such clumps of $r_{\text{Cl}} \sim 0.1$ pc. Since this size is consistent with our observed scale ($\lesssim 0.4$ pc), one might speculate that light from distinct clumps may contribute to our observed flux. Such dust clumps can also exist in polar direction at similar distances from the nucleus. Another possibility is that free electrons located above and below the broad-line emission region in the ionization cone at distances of only a fraction of a parsec scatter central light into our line-of-sight.

It has already been discussed by Wittkowski et al. (1998) that a fraction of the K -band photons originating from the central engine could reach us directly through only moderate extinction in the near-infrared, despite the Seyfert 2 type of this AGN. The A_V could be as low as ~ 10 m (Bailey et al. 1988), corresponding to $A_K \sim 1.2$ m assuming standard galactic extinction. With the concept of a clumpy torus, the chance of low extinction towards the central source is even larger than for a smooth dust distribution. In this case, an analysis of the separated flux spectrum of only the very compact ($\lesssim 5$ mas) component should reveal a type 1 spectrum, which is supported by the possible detection of a broad Br γ line by Gratadour et al. (2003). Non-negligible K -band flux contributions of the order of a few hundred milli-Jansky could arise from the central accretion flow (cf. Wittkowski et al. 1998; Beckert & Duschl 2002; Weigelt et al. 2004). Stars are very unlikely to contribute significantly to the K -band flux on scales $\lesssim 0.4$ pc (see e.g., Thatte et al. 1997).

Comparison to VLTI/MIDI NGC 1068 and Keck NGC 4151 observations. It is striking that the two NGC 1068 K -band scales found by our VLTI/VINCI observations and by speckle interferometry (Wittkowski et al. 1998; Weigelt et al. 2004) of $\lesssim 0.4$ pc and about 2×4 pc, respectively, are very similar to those of the two NGC 1068 dust components reported by Jaffe et al. (2004) based on the N -band VLTI/MIDI observations. The latter include a hot ($T > 800$ K) $0.8 \times (< 1)$ pc and a warm ($T \sim 320$ K) $\sim 2.5 \times 4$ pc component. Hot thermal emission from inner substructure of the dusty torus, as well as direct light from the central accretion flow could explain the K -band as well as the N -band very compact sub-parsec component. It is unlikely, though, that the warm VLTI/MIDI component and the 2×4 pc K -band component can be explained by the same dust component.

The Keck Interferometer observations of the *Seyfert 1* nucleus of NGC 4151 (Swain et al. 2003) showed that the majority of the central (~ 3 pc) K -band light arises from very small scales of $\lesssim 0.1$ pc, probably from the central accretion disk. Our K -band observations of the *Seyfert 2* galaxy NGC 1068 show that only part of the central light arises from compact $\lesssim 0.4$ pc scales while another part arises from larger scales. This difference is in line with the unified scheme which predicts that the central engine of Seyfert 2 cores is obscured, which leads to a larger (up to 100%) relative flux contribution from surrounding material.

4. Conclusion

We have obtained K -band interferometric observations of the nucleus of the Seyfert 2 galaxy NGC 1068, and hereby show

that the correlated magnitude of this AGN up to a baseline of at least ~ 50 m is such that it can be studied with the VLTI at near-infrared wavelengths.

Together with other observations, we conclude that a K -band flux of $\gtrsim 50$ mJy originates from scales clearly smaller than about 5 mas or 0.4 pc and another part of the flux from larger scales. Our VLTI/VINCI measurement alone sets an upper limit of ≤ 6.7 mas at the 3σ level to the Gaussian $FWHM$ of the very compact component. The origin of this newly constrained small-scale emission can be interpreted as substructure of the dusty torus, as for instance part of a clumpy inner cavity or distinct clumps forming the torus, or as direct emission from the central accretion flow viewed through only moderate extinction in the K -band.

Acknowledgements. The VLTI observations reported here were made possible through the efforts of the whole ESO VLTI and MACAO commissioning teams.

References

- Antonucci, R. R. J., & Miller, J. S. 1985, ApJ, 297, 621
 Antonucci, R. R. J. 1993, ARA&A, 31, 473
 Arsenault, R., Alonso, J., Bonnet, H., et al. 2003, The Messenger, 112, 7
 Bailey, J., Axon, D. J., Hough, J. H., et al. 1988, MNRAS, 234, 899
 Barvainis, R. 1987, ApJ, 320, 537
 Beckert, T., & Duschl, W. J. 2002, A&A, 387, 422
 Bland-Hawthorn, J., Gallimore, J. F., Tacconi, L. J., et al. 1997, Ap&SS, 248, 9
 Bock, J. J., Neugebauer, G., Matthews, K., et al. 2000, AJ, 120, 2904
 Bordé, P., Coudé du Foresto, V., Chagnon, G., & Perrin, G. 2002, A&A, 393, 183
 Claret, A. 2000, A&A, 363, 1081
 Cohen, M., Walker, R. G., Carter, B., et al. 1999, AJ, 117, 1864
 Dopita, M. A., Heisler, C., Lumsden, S., & Bailey, J. 1998, ApJ, 498, 570
 Efstathiou, A., & Rowan Robinson, M. 1995, MNRAS, 273, 649
 Granato, G. L., & Danese, L. 1994, MNRAS, 268, 235
 Gratadour, D., Clénet, Y., Rouan, et al. 2003 A&A, 411, 335
 Jaffe, W., Meisenheimer, K., Röttgering, H. J. A., et al. 2004, Nature, in press
 Kervella, P., Coudé du Foresto, V., Glindemann, A., & Hofmann, R. 2000, Proc. SPIE, 4006, 31
 Kervella, P., Gitton, Ph., & Ségransan, D., et al. 2003, Proc. SPIE, 4838, 858
 Kervella, P., Ségransan, D., & Coudé du Foresto, V. 2004, A&A, submitted
 Krolik, J. H., & Begelman, M. C. 1988, ApJ, 329, 702
 Manske, V., Henning, T., & Men'shchikov, A. B. 1998, A&A, 331, 52
 Nenkova, M., Ivezić, Z., & Elitzur, M. 2002, ApJ, 570, L9
 Pier, E. A., & Krolik, J. H. 1992, ApJ, 401, 99
 Rouan, D., Rigaut, F., Alloin, D., et al. 1998, A&A, 339, 687
 Swain, M., Vasisht, G., Akeson, R., et al. 2003, ApJ, 596, L163
 Thatte, N., Quirrenbach, A., Genzel, R., et al. 1997, ApJ, 490, 238
 Vollmer, B., Beckert, T., & Duschl, W. J. 2004, A&A, 413, 949
 Weinberger, A. J., Neugebauer, G., & Matthews, K. 1999, AJ, 117, 2748
 Wittkowski, M., Balega, Y., Beckert, T., et al. 1998, A&A, 329, L45
 Wittkowski, M., Duschl, W. J., Hofmann, K.-H., et al. 2003, Proc. SPIE, 4838, 1378
 Weigelt, G., Wittkowski, M., Balega, Y. Y., et al. 2004, A&A, submitted